

Mesothelin overexpression promotes autocrine IL-6/sIL-6R trans-signaling to stimulate pancreatic cancer cell proliferation

Uddalak Bharadwaj¹, Christian Marin-Muller^{1,2},
Min Li^{1,3}, Changyi Chen¹ and Qizhi Yao^{1,2,*}

¹Molecular Surgeon Research Center, Michael E. DeBakey Department of Surgery and ²Department of Molecular Virology and Microbiology, Baylor College of Medicine, Houston, TX 77030, USA and ³Present address: The Vivian L. Smith Department of Neurosurgery, The University of Texas Health Science Center at Houston, Medical School, 6431 Fannin Street, MSB 3.000 Houston, TX 77030, USA

*To whom correspondence should be addressed. Michael E. DeBakey Department of Surgery, Baylor College of Medicine, One Baylor Plaza, Mail stop BCM 391, Houston, TX 77030, USA. Tel: +1 713 798 1765, Fax +1 713 798 6633; Email: qizhiyao@bcm.edu

Mesothelin (MSLN) overexpression in pancreatic cancer (PC) leads to enhanced cell survival/proliferation and tumor progression. After screening for a number of growth factors/cytokines, we found that the MSLN expression correlated closely with interleukin (IL)-6 in human PC specimens and cell lines. Stably overexpressing MSLN in different PC cell lines (MIA-MSLN and Panc1-MSLN) led to higher IL-6 production. Silencing MSLN by small interfering RNA (siRNA) significantly reduced IL-6 levels. Blocking the observed constitutive activation of nuclear factor-kappaB (NF-κB) with IKK inhibitor wedelolactone in MIA-MSLN cells also reduced IL-6. Silencing IL-6 by siRNA reduced cell proliferation, cell cycle progression and induced apoptosis with significant decrease of c-myc/bcl-2. Interestingly, recombinant IL-6-induced proliferation of MIA-MSLN cells but not MIA-V cells. Although messenger RNA/protein levels of IL-6R did not vary, soluble IL-6R (sIL-6R) was significantly elevated in MIA-MSLN and was reduced by treatment with the TACE/ADAM17 inhibitor TAPI-1, indicating intramembrane IL-6R cleavage and IL-6 trans-signaling may be operative in MIA-MSLN cells. Blocking the IL-6/sIL-6R axis using sIL-6R antibody abrogated basal proliferation/survival as well as recombinant human IL-6-induced cell proliferation. Our data suggest that MSLN-activated NF-κB induces elevated IL-6 expression, which acts as a growth factor to support PC cell survival/proliferation through a novel auto/paracrine IL-6/sIL-6R trans-signaling. In addition, using a panel of PC cells with varying MSLN/IL-6 expressions, we showed that MSLN/IL-6 axis is a major survival axis in PC supporting tumor cell growth under anchorage-dependent and independent conditions. The close correlation between MSLN and IL-6 provides a new rationale for combination therapy for effective control of MSLN-overexpressing PCs.

Introduction

The glycosphosphatidylinositol (GPI) anchored glycoprotein mesothelin (MSLN), is validated as a preferred immunotherapeutic target in pancreatic cancer (PC), ovarian cancer and mesothelioma (1,2), yet the role of MSLN in pathogenesis of these and other cancers has only started to unfold. Overexpressed MSLN increases PC cell proliferation under reduced serum conditions through an activated Stat3 pathway (2,3). High MSLN appears to confer a protective effect against anoikis in breast cancer (4). Further detailed study of the mechanism of MSLN involvement in PC survival/pathogenesis is desired.

Abbreviations: FBS, fetal bovine serum; HPDE, human pancreatic ductal epithelial; IL, interleukin; mRNA, messenger RNA; MSLN, mesothelin; MTT, 3-(4,5-dimethylthiazole-2-yl)-2,5-biphenyl tetrazolium bromide; NF-κB, nuclear factor-kappaB; PC, pancreatic cancer; rIL-6, recombinant human interleukin-6; siRNA, small interfering RNA; TNF, tumor necrosis factor.

Cancer cells often upregulate growth/survival pathways through autocrine production of growth factors. Recent studies point toward interleukin (IL)-6 as an important tumor-promoting autocrine (5,6) and anti-apoptotic (7,8) factor in cancer. Clinical studies have shown elevated serum IL-6 concentrations in cancer patients (9), including those with PC (10,11), and serum IL-6 levels correlate with tumor stage, survival, metastasis and cachexia in several malignancies (9). Autocrine IL-6 is implicated as an important activator of oncogenic Stat3 in lung adenocarcinomas (6) and PC (12). IL-6 in PC is also found to promote proliferation, cell survival (10,13), and resistance to radiation-induced apoptosis (14). About 15–20% of cancers are attributable to infection and/or inflammation including hepatocellular cancer (hepatitis B or C infections), gastric cancer (*Helicobacter pylori* infection), colorectal cancer (Inflammatory Bowel Disease (IBD)), PC (chronic pancreatitis) and many more (15), and IL-6 seems to play a major role by promoting various hallmarks of neoplastic transformation such as growth factor independence, apoptosis resistance and angiogenesis (9,16). The IL-6-Stat3 axis seems to promote colitis-associated tumorigenesis (17,18). In addition, IL-6 is a known autocrine growth factor for mesothelial cells (19), the only normal cells that express MSLN. In our previous studies, we have found that Stat3 is activated in MSLN overexpressing cells (3). Suppressed Stat3 activation was also observed in expressed in renal carcinoma (ERC, rat homologue of MSLN) deficient cells (20).

Although there have been studies on IL-6 in PC, no studies have shown the function of IL-6 in correlation with MSLN overexpression in PC cells. In this study, we examined the hypothesis that MSLN overexpression in pancreatic tumor cells activates NF-κB and results in secretion of high levels of IL-6, which could in turn be responsible for the cells' increased viability and proliferation under serum-reduced conditions through a IL-6/soluble IL-6R (sIL-6R) trans-signaling mechanism.

Material and methods

Cell culture, chemicals, antibodies and human tissue specimens

Human PC cell lines, MIA PaCa-2, Panc-1, SU.86.86, Panc 03.27, Capan-1, CFPAC-1, BxPC-3, PL45, Hs766T, HPAF-II, AsPC-1 and Capan-2 were purchased from American Type Culture Collection (ATCC, Rockville, MD). Human pancreatic ductal epithelial cells (HPDE) were a gift from Dr Ming-Sound Tsao (Ontario Cancer Institute, Toronto, ON). Puromycin and anti-β-actin antibody were purchased from Sigma (St Louis, MO). Other antibodies were from multiple sources: p-IκB-α, IκB-α, p-IKK-α/β, IKK-α, Caspase3, c-myc, Mcl-1, pStat3 (Tyr 705), Bcl-2, goat anti-rabbit IgG (H&L) antibody-horseradish peroxidase and goat anti-mouse IgG (H&L) antibody-horseradish peroxidase from Cell Signaling Technology Laboratories (Beverly, MA); p65 from Santa Cruz Biotechnology (Santa Cruz, CA); antibodies to IL-6 and sIL-6R from R&D Systems and lamin A antibody from Abcam (Cambridge, MA). Human pancreatic adenocarcinoma specimens were collected from patients, who underwent surgery according to an approved human protocol at Baylor College of Medicine (Houston, TX).

Bio-Plex IL-6 assay

The concentration of IL-6 in cell supernatants and PC patient sera was determined using the Bio-Plex human IL-6 Assay kit (Bio-Rad Laboratories, Hercules, CA) according to the manufacturer's protocol. Briefly, 50 μl of the supernatant/cytokine standard was added to the plate coated with beads coupled to IL-6 antibody. After a series of washes, a biotinylated detection antibody, specific for a different IL-6 epitope was added to the reaction resulting in formation of antibodies assimilated around the target protein. Streptavidin-phycoerythrin (streptavidin-PE) was then added to bind to the biotinylated detection antibody on the bead surface. The data from the reaction were analyzed by using Bio-Plex suspension array system (or Luminex 100 system) from Bio-Rad Laboratories.

Real-time polymerase chain reaction

MSLN, IL-6, IL-6R and sIL-6R (alternatively spliced form), ADAM10, ADAM17 and GAPDH messenger RNA (mRNAs) were analyzed by real-time reverse

transcription–polymerase chain reaction using the SYBR Green supermix kit (Bio-Rad Laboratories) as described previously (2). The relative mRNA levels were normalized to GAPDH mRNA and presented as unit values of $2^{-C_t(\beta\text{-actin})-C_t(\text{gene of interest})}$, where C_t is threshold cycle. Primer sequences for the genes are as follows: h-IL-6 sense: 5'-TCCAGAACAGATTTGAGAGTAGTG-3'; h-IL-6 antisense: 5'-GCATTTGTGGTTGGGTCAGG-3'; h-sIL-6R-sense: 5'-GCGA-CAAGCCTCCCAGGTTTC-3'; h-sIL-6R-antisense: 5'-GTGCCACCCAGCCAGCTATC-3'; hADAM17-sense: 5'-GGTGGTAGCAGATCATCGCTT-3'; hADAM17-antisense: 5'-GTGGAGACTTGAGAATGCGAA-3'; hADAM10-sense: 5'-ATGGGAGTCCAGTATGGGAATC-3' and hADAM10-antisense: 5'-TTTGGCACGCTGGTGTTTTTG-3'.

MSLN/IL-6 shRNA/small interfering RNA transfections

For MSLN shRNA transfection experiments, a plasmid encoding MSLN shRNA (TR311377; Origene, Rockville, MD) and a control plasmid encoding GFP shRNA (TR30003) were used. MIA-MSLN/MIA-V cells were transfected with the above or an MSLN-specific small interfering RNA (siRNA) oligonucleotide or a pool of four human IL-6-specific siRNA oligonucleotides (IL-6 siRNA Pool #1; Thermo Scientific, IL) using Lipofectamine 2000 (Invitrogen, CA). Negative controls included cells treated with transfection reagent (mock) and control scramble siRNA (for MSLN siRNA experiments) or a pool (Non-Targeting siRNA Pool #1; Thermo Scientific) of scrambled siRNAs (for IL-6 siRNA experiments). Cells/supernatants were collected 24/48 h after transfection for mRNA/protein extraction for real-time polymerase chain reaction/Bio-Plex detection and functional studies done as indicated.

Immunoblot analysis

Cells were lysed in lysis buffer (Cell Signaling Technology Laboratories) with phosphatase and protease inhibitors. Total proteins (60 μg) were resolved by sodium dodecyl sulfate–polyacrylamide gel electrophoresis and transferred to nitrocellulose membrane (Bio-Rad Laboratories). Different proteins were detected using specific primary antibodies, appropriate horseradish peroxidase-conjugated secondary antibodies and the ECL detection system (GE Healthcare Bio-Sciences Corp., Piscataway, NJ). Nuclear/cytoplasmic extracts were prepared using N-PER reagents (Pierce Biotechnology, Rockford, IL) and used for studying nuclear translocation of p65. For detecting sIL-6R in the supernatant, protein from serum-free supernatants were acetone-precipitated overnight at -20°C , solubilized in protein loading dye and subjected to immunoblot analysis.

Treatment with inhibitors

MIA-MSLN/MIA-V cells were treated with 0, 12.5 or 25 μM of the IKK inhibitor wedelolactone (Calbiochem, La Jolla, CA). Cells were collected after 24 h and whole cell and cytoplasmic/nuclear extracts were prepared according to procedures already described (21) and used for western blot. Supernatants were collected for Bio-Plex detection of secreted IL-6. After a 36 h serum starvation, TAPI-1, the TACE inhibitor was used at 10–20 μM final concentration for 36 h (for sIL-6R in supernatant) and 4 days [to check proliferation by 3-(4,5-dimethylthiazole-2-yl)-2,5-biphenyl tetrazolium bromide (MTT)].

Cell proliferation measurement by cell viability assay (MTT)

Cell proliferation was determined by measuring cell viability using MTT. Briefly, 2000 cells were plated and serum starved for 24 h. Serum free or 0.2% serum media \pm treatments were added to the plates and the cells were continuously cultured for 2, 3 or 6 days and viability measured by MTT. Optical density (OD) was measured at 590 nm using a 96-well multi-scanner (EL-800 universal microplate reader; BioTek, Winooski, VT). Proliferating capacity of a cell was measured by dividing its viability at a certain time point by its viability at 0 day (day after plating cells). For antibody blocking experiments, anti-sIL-6R Abs or isotype control Abs were added to the starvation media at a final concentration of 5 or 25 $\mu\text{g}/\text{ml}$. Further treatment with serum free or 0.2% serum media plus other treatments were added the next day while maintaining antibody concentrations. After 3 days, viabilities were measured as indicated above. To study effect of IL-6 siRNA on MIA-MSLN proliferation, MIA-MSLN/MIA-V cells were transfected using IL-6-specific siRNA pool or negative control non-targeting siRNA pool in six-well plates. The next day cells were trypsinized, and 4000 cells were plated in replicate in 96-well plates and serum starved for 24 h. Fresh medium with 0.2% serum was added to the plates and continuously cultured for another 48 h, and the viability was measured by MTT as above. For IL-6 treatment experiment, IL-6 was used at 0.1, 1, 10 or 100 ng/ml. For the combined IL-6 and sIL-6R treatment, IL-6 and sIL-6R were used at concentrations of 100 ng/ml and 2 $\mu\text{g}/\text{ml}$, respectively.

Cell cycle analysis

Cells were harvested and processed using the CycleTEST™ PLUS DNA Reagent Kit from Beckton Dickinson (San Jose, CA) according to the manufacturer's

instructions. Flow cytometry [fluorescence-activated cell sorting (FACS)] analysis was carried out to examine the cell cycle distribution by a FACSCalibur (Becton Dickinson). Data were further analyzed using the software FLOWJOW Ver. 6.1.1 (Tree Star, San Carlos, CA).

Reverse transfection to study effect of MSLN/IL-6 siRNA on growth of cells under anchorage-dependent and independent conditions

Cell lines were transfected with pools of MSLN/IL-6-specific siRNA or non-targeting scrambled siRNA and plated as per reverse transcription protocol in full growth medium in 96-well plates, in triplicates. After 36 h, cells were serum starved for 24 h prior to continued culture for 5 days in 0.2% serum containing media. Relative viability was measured by dividing viability of treated cells (treated with IL-6/MSLN/scrambled siRNA) by that of mock-treated cells using MTT assay. For anchorage-independent spheroid cultures, 36 h posttransfection, cells were trypsinized and plated at 6000 cells per well of ultra-low attachment 96-well plates and cultured for 5 days before being photographed using phase contrast microscopy or viability measured by MTT.

Results

High MSLN-expressing PC cell lines secrete high levels of IL-6

The correlation of secreted IL-6 levels with high MSLN expression in PC was studied using a small panel of different PC cell lines, including MIA PaCa-2, Panc-1, BxPC-3 and HPDE cells. Shown in Figure 1A, HPDE, MIA PaCa-2 and Panc-1 cells showed lower IL-6 levels in the culture supernatant, and these cells also express low levels of MSLN at both mRNA (Figure 1B) and protein levels (2) when compared with BxPC-3, a cell line showing very high expression of MSLN and high IL-6 production. The IL-6 level in the BxPC-3 culture medium was 5–17 times higher than the other cells. These data indicated a positive correlation between MSLN expression and IL-6 production in PC cell lines. To examine a more extensive spectrum of PC cell lines for MSLN and IL-6 expression profile, we further screened 15 cells which include 14 PC cell lines and a control HPDE cell for MSLN and IL-6 mRNA expression (summarized in Table I). When compared with HPDE cells, there are eight cell lines, which show both high MSLN expression (>3 -fold over HPDE) and IL-6 expression (>10 -fold over HPDE) and three cell lines which show low MSLN and low IL-6. There are also some cell lines that do not fall in either category such as two cell lines with low MSLN but high IL-6 (Panc28/SU86.86) and two cell lines with high MSLN but low IL-6 (AsPC-1/Capan-2). These data showed that the majority of the PC cell lines tested followed the pattern of positive association of MSLN and IL-6 expression.

Serum IL-6 levels in PC patients positively correlate with the level of MSLN expression in the cancer tissue

To further test the MSLN-IL-6 correlation, we examined serum IL-6 levels in six PC patients using the Bio-Plex assay. The tumor/normal tissue ratio of MSLN expression showed a high correlation with the serum IL-6 level ($r = 0.982$, $P < 0.001$, Figure 1C). The mean IL-6 level in these patients was 7.2 ± 4 pg/ml, which was higher than the previously reported (mean IL-6 level 3.4 pg/ml) in PC patients (22).

Forced overexpression of MSLN in PC cell lines leads to enhanced IL-6 production

Our previous study showed that MSLN overexpressing stable MIA PaCa-2 cells (MIA-MSLN) had increased migration and proliferation under serum-reduced conditions (2,3). To decipher the mechanism of these enhanced functions, we studied the MIA-MSLN cell line in detail for expression of various growth factors, cytokines and their receptors (data not shown). We found that the MIA-MSLN cell line secreted ~ 18 times higher quantity of IL-6 compared with untransfected (MIA), vector control, (MIA-V) and GFP-expressing control cells (MIA-GFP) (Figure 2A, $P < 0.01$). Similarly, IL-6 mRNA was also significantly higher in MIA-MSLN cells than in MIA-V cells ($P < 0.01$) (Figure 2B). When we blocked MSLN expression (Figure 2C, $P < 0.05$) in MIA-MSLN cells using specific shRNA/siRNA against MSLN, the IL-6 expression level was drastically reduced at the mRNA level (Figure 2B, $P < 0.01$) and protein level (Figure 2D, $P < 0.05$). These data strongly suggest that

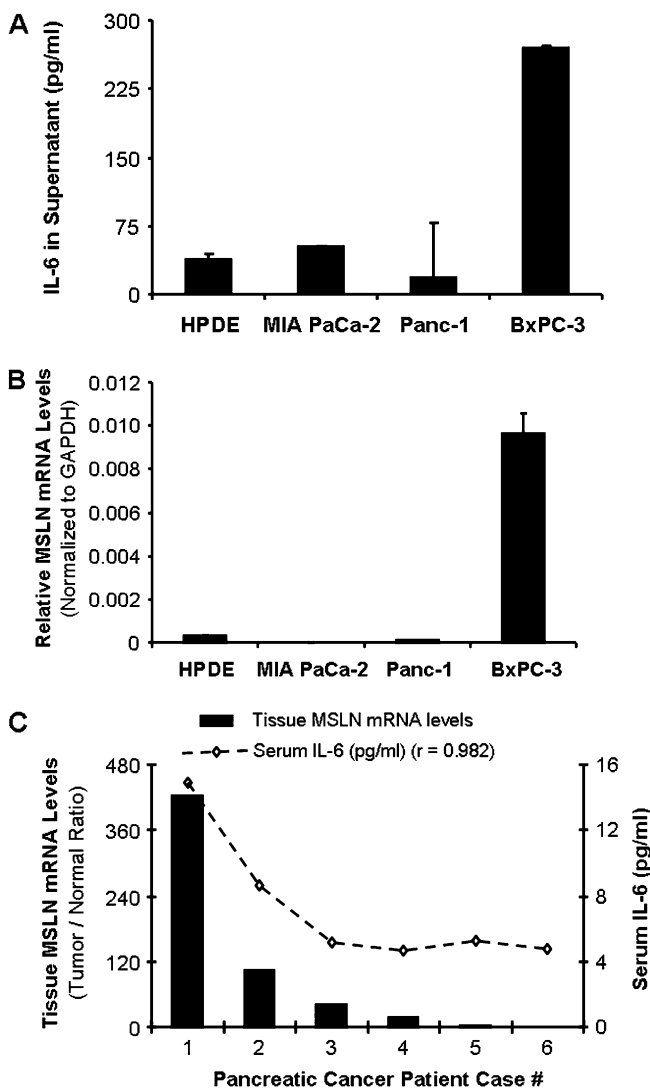


Fig. 1. MSLN expression level correlates well with IL-6 expression in PC cell lines and tissues. (A) IL-6 levels in PC cell lines MIA PaCa-2, Panc-1, BxPC-3 and HPDE cells. Cells were seeded at 1×10^6 cells per well in six-well plates and cultured until 60% confluence. Thereafter, the medium was replaced and the supernatants were harvested at 48 h of further incubation and tested for IL-6 using the Luminex-based IL-6 assay kit. Values on Y-axis show the amount of IL-6 in pg/ml, bars denoting standard deviation (SD) of duplicate data. (B) Relative MSLN mRNA levels in PC cell lines MIA PaCa-2, Panc-1, BxPC-3 and HPDE cells. Total mRNA from the cell lines were reverse transcribed and tested for MSLN expression. The results depicted denote MSLN mRNA levels in each cell line normalized to the GAPDH mRNA level. Relative mRNA level is presented as $2^{-[C_t(\text{GAPDH}) - C_t(\text{MSLN})]}$ and is representative of at least two independent experiments. The bars denote SD of duplicate data. (C) Sera from six PC patients were tested for secreted IL-6 using Bioplex cytokine kit. Paired tumor and normal tissues (T/N) from the same patients were tested for the expression of MSLN mRNA by using real-time polymerase chain reaction and represented by the bar graph. The left hand side Y-axis denotes T/N ratio of the GAPDH-normalized MSLN mRNA levels. Line graph represents the serum IL-6 level in six patient samples and the right hand side Y-axis indicates IL-6 concentrations in pg/ml.

MSLN expression leads to increased IL-6 production in PC cells. We also tested a second MSLN overexpressing stable cells line Panc-1, for IL-6 production. Figure 2E shows that the Panc-1-MSLN cells expressed significantly higher ($P < 0.01$) MSLN than the control cells. Just like the MIA-MSLN cells, the Panc-1-MSLN cells also expressed significantly higher quantities of IL-6 mRNA compared with untransfected (Panc-1), vector control cells (Panc-1-V), and GFP-expressing control cells (Panc-1-GFP) (Figure 2F, $P < 0.01$).

Table I. MSLN and IL-6 mRNA expression in a panel of PC cell lines

	MSLN (>3-fold over HPDE)	IL-6 (>10-fold over HPDE)
HPDE	—	—
MIA PaCa-2	—	—
Panc-1	—	—
Panc28	—	+
SU.86.86	—	+
Panc 03.27	+	+
Capan-1	+	+
CFPAC-1	+	+
BxPC3	+	+
PL45	+	+
Hs766T	+	+
HPAF-II	+	+
Panc48	+	—
AsPC-1	+	—
Capan-2	+	—

MSLN-induced NF- κ B activation is responsible for the high IL-6 secretion in MIA-MSLN cells

Various reports indicated that aberrantly activated NF- κ B leads to induction of IL-6 in many cancers (23), including PC. We examined NF- κ B activation in the MIA-MSLN cells and control MIA-V cells and found that nuclear translocation of NF- κ B was indeed substantially increased in MIA-MSLN cells (Figure 3A). We could block this increased p65 nuclear translocation with a specific IKK blocker, wedelolactone, with a corresponding decrease in the phosphorylated as well as total I κ B- α in the cytoplasm of treated MIA-MSLN cells (Figure 3A). We then measured IL-6 in the supernatants from the MIA-V and MIA-MSLN cells treated with wedelolactone using Bio-Plex. We found that blocking NF- κ B activation decreased the secretion of IL-6 significantly from 251.4 pg/ml in the untreated MIA-MSLN cells to 117 pg/ml (a 53% reduction) and 75 pg/ml (a 70% reduction) (Figure 3B, $P < 0.01$) in cells treated with 12.5 and 25 μ M of wedelolactone, respectively. These data show that MIA-MSLN cells have aberrantly activated NF- κ B, which leads to an increased production of the inflammatory cytokine IL-6.

Increased IL-6 in MIA-MSLN cells is responsible for their enhanced survival and proliferation under serum-reduced conditions in an autocrine manner

A number of studies have indicated a growth-promoting property of IL-6 in various cancer cells (5,24–27). IL-6 has been reported as both an autocrine and paracrine factor supporting growth factor independence and/or lower growth factor requirement for cancer cells. We found that MIA-MSLN cells proliferated more than control MIA-V cells, even in serum-free medium. MTT assay showed that MIA-MSLN cells proliferated almost 1.8 times faster than the MIA-V cells after day 4 ($P < 0.01$) and almost 2.6 times faster at day 6 ($P < 0.01$, Figure 4A). Clearly, MIA-MSLN cells had a lesser requirement for growth factors for their growth. We observed that MIA-MSLN cells, which secreted high IL-6, produced even higher quantities of IL-6 while on starvation. After 24 h of starvation, the MIA-MSLN cells produced \sim 590 pg/ml of IL-6 and 48 h of serum deprivation increased the concentration of IL-6 in the supernatant to 3029 pg/ml (Figure 4B). However, MIA-V cells produced only negligible amounts of the cytokine IL-6 at all time points. This indicated that IL-6 could be responsible for the growth factor-independent survival/growth of these cells. We then used specific siRNA against IL-6 to block IL-6 expression and observe its effect on cell proliferation. Figure 4C clearly shows that IL-6 siRNA significantly reduced proliferation of MIA-MSLN cells ($P < 0.01$) to a rate similar to that of MIA-V cells after 2 days in 0.2% fetal bovine serum (FBS) containing media. We then examined whether IL-6 affects cell proliferation or survival. As shown in Figure 4D, 24 h IL-6 siRNA treatment significantly ($P < 0.05$) reduced S phase cells from 33 (mock transfected) and 29%

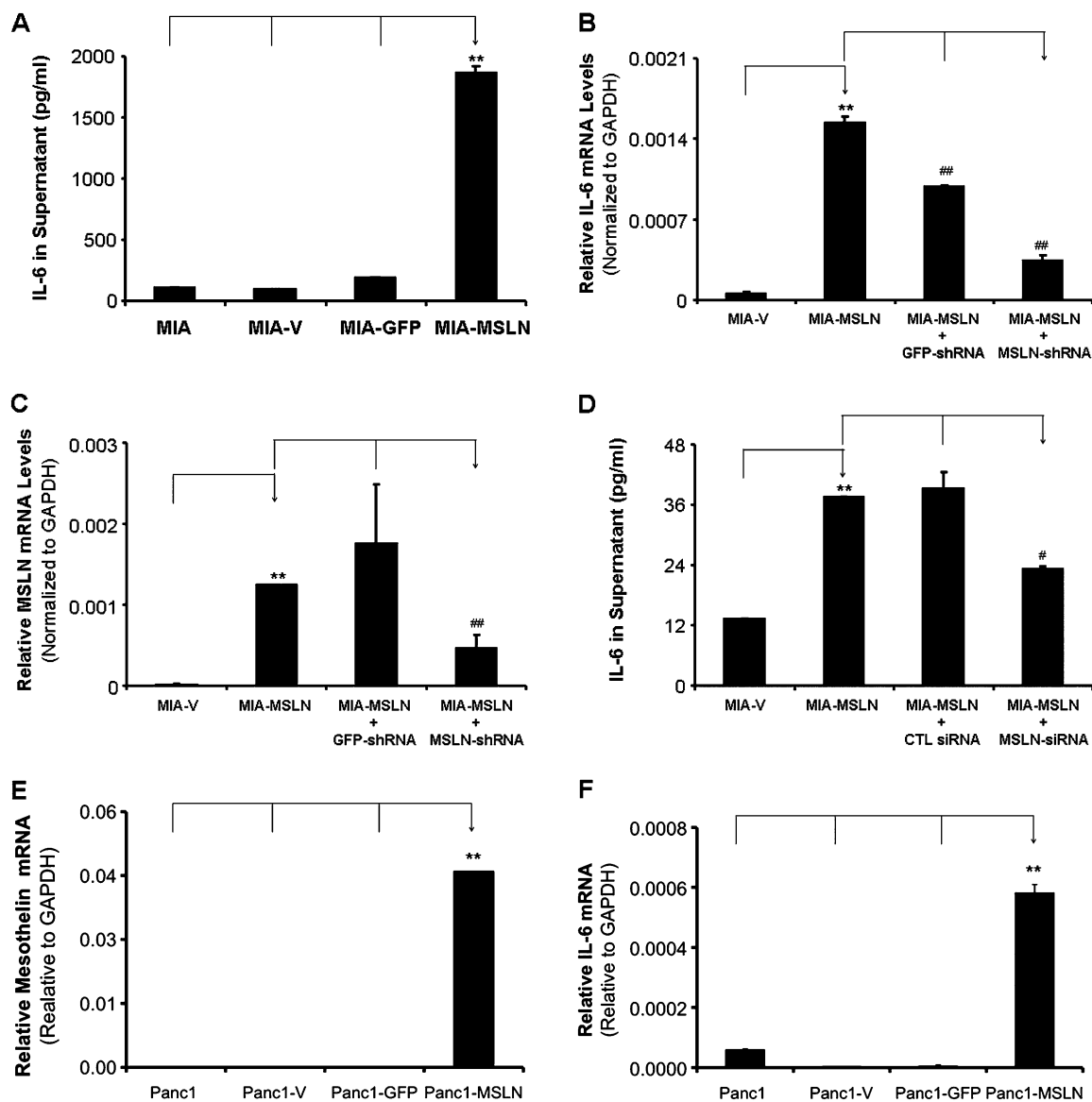


Fig. 2. MSLN overexpression leads to increased IL-6 production in PC cells. (A) MIA, MIA-V, MIA-GFP and MIA-MSLN cells were seeded at 1×10^6 cells per well in six-well plates and cultured until 60% confluence. Thereafter, the medium was replaced and the supernatants were harvested at 48 h of further incubation and the levels of IL-6 were determined by using the Luminex-based IL-6 assay kit. Y-axis represents IL-6 concentration in pg/ml. (B) Silencing MSLN using MSLN-specific shRNA plasmid. MIA-V and MIA-MSLN cells were transfected with MSLN-specific shRNA plasmids or GFP shRNA control plasmids. The cells collected 48 h posttransfection were used to detect MSLN mRNA by real-time polymerase chain reaction. The MSLN-expressing levels were detected by using real-time polymerase chain reaction. Y-axis represents MSLN mRNA level normalized to the GAPDH mRNA level. Relative mRNA level is presented as $2^{-[C_t(\text{GAPDH}) - C_t(\text{IL-6})]}$. The bars denote SD of duplicate data. Experiment was performed several times using separate MIA-MSLN pools and different siRNA/shRNAs against MSLN with similar results. (C) Silencing MSLN decreases IL-6 mRNA production in MIA-MSLN cells. MIA-V and MIA-MSLN cells were transfected with MSLN-specific shRNA plasmids or GFP shRNA control plasmids. The cells collected 48 h posttransfection were used to detect IL-6 mRNA by real-time polymerase chain reaction. Y-axis represents IL-6 mRNA level relative to GAPDH. The bars denote SD of duplicate data. Experiment was performed several times using separate MIA-MSLN pools and different siRNA/shRNAs against MSLN with similar results. (D) Silencing MSLN decreases IL-6 secretion in MIA-MSLN cells. MIA-V and MIA-MSLN cells were transfected with MSLN-specific siRNA or scrambled siRNA. The cells collected 48 h posttransfection from 24-well plates in 2 ml of medium were used to detect IL-6 by Luminex-based IL-6 assay kit. Values on Y-axis show the amount of IL-6 in pg/ml, bars denoting SD of duplicate data. (E) Stable overexpression of MSLN in human PC cell Panc1. The GAPDH-normalized MSLN expression levels in the stably MSLN expressing (Panc1-MSLN) and control MIA cells generated by retroviral gene transfer and subsequent puromycin selection are shown. (F) Panc1, Panc1-V, Panc1-GFP and Panc1-MSLN cells were seeded at 1×10^6 cells per well in six-well plates and cultured until 80% confluence, cells collected were used to detect IL-6 mRNA by real-time polymerase chain reaction. Y-axis represents IL-6 mRNA level relative to GAPDH. The bars denote SD of duplicate data. *, # denote $P < 0.05$, and **, ## denote $P < 0.01$, compared with controls, *t*-test. * and # denote comparison to different base lines and hence are denoted differently.

(scrambled siRNA control) to 21%. Simultaneously, we saw a leap in G_1 cells (68%) compared with only 51% in mock-transfected cells. Next, we examined apoptosis induction by IL-6-blocking at day 5. Figure 4E clearly shows under serum-free conditions, MIA-V cells underwent apoptosis as indicated by decreased intact (uncleaved) caspase3, whereas the MIA-MSLN cells were relatively viable.

siRNA against IL-6 on the other hand clearly decreased survival of MIA-MSLN cells with increased cleavage of caspase3. We then checked a number of pro- and anti-apoptotic proteins regulated by IL-6/stat3 pathway and found reasonable reduction in levels of the anti-apoptotic mcl-1 and bcl-2 as also the c-myc protein (Figure 4F), indicating a major role of these in MIA-MSLN cell survival.

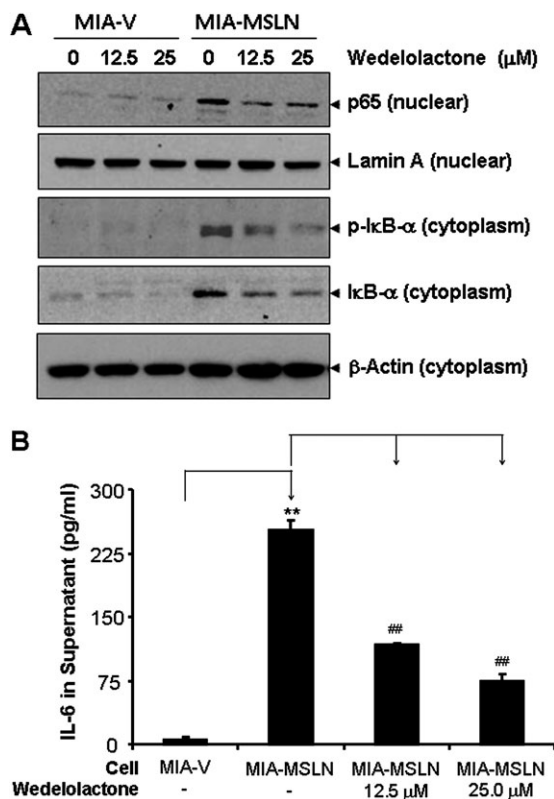


Fig. 3. Blocking NF- κ B activation in MIA-MSLN cells leads to decrease in IL-6 expression. (A) NF- κ B activation in MIA-MSLN cells was blocked by IKK inhibitor wedelolactone. For the nuclear extract, 20 μ g of nuclear total proteins from control MIA-V and MIA-MSLN cells treated with or without IKK inhibitor wedelolactone at the indicated concentrations for 24 h was subjected to immunoblot analysis with antibodies against p65 and lamin A. For the cytosolic proteins, 30 μ g of cytoplasmic protein from the same cells were subjected to immunoblot for p-I κ B α , I κ B α and β -actin. Data from a representative blot is shown. (B) Blocking NF- κ B activation by wedelolactone reduced IL-6 production in MIA-MSLN cells. At 48 h posttreatment with wedelolactone in MIA-V and MIA-MSLN cells at the indicated concentrations, the supernatants were collected and tested for IL-6 using the Luminex-based IL-6 assay kit. Values on Y-axis show the amount of IL-6 in pg/ml, bars denoting SD of duplicate data. *, # denote $P < 0.05$, and **, ## denote $P < 0.01$, compared with controls, t -test.

Exogenous IL-6 can stimulate MIA-MSLN cell proliferation with upregulated soluble IL-6 receptor but not surface IL-6 receptor

Because IL-6 seemed to act in an autocrine fashion to support MIA-MSLN cell survival/proliferation, we examined whether exogenous IL-6 could induce MIA-MSLN growth. Treatment with increasing concentrations (0, 0.1, 1, 10 or 100 ng/ml) of recombinant human IL-6 (rIL-6) did not have any effect on the growth of control cells (Figure 5A). However, rIL-6 significantly increased proliferation of MIA-MSLN cells at 10 and 100 ng/ml (Figure 5A, $P < 0.01$).

To study why IL-6 failed to induce growth in control cells, we examined expression of the two receptors involved in IL-6 signaling, the specific IL-6R gp80 and the signal-transducing partner, gp130. The mRNA level of gp80 (IL-6R) was low in both cells (Figure 5B). FACS analysis using anti-gp80 antibody that could detect membrane-bound IL-6 receptor (mIL-6R), revealed both cells had low mIL-6R expression, although it was marginally elevated in MIA-MSLN cells (Figure 5C, a). Western blotting using a IL-6R (alpha chain)-specific antibody revealed elevated levels of a lower molecular weight band at ~ 50 kD, consistent with a sIL-6R, in supernatants from serum starved MIA-MSLN cells but not MIA-V cells, (Figure 5C, b). This suggested the interesting possibility that IL-6/sIL-6R trans-signaling was involved.

sIL-6Rs could be generated by two mechanisms: by alternatively spliced mRNA for p80 or by intramembrane enzymatic cleavage by metalloproteinases ADAM10 (TACE) and ADAM17 (28). To ascertain the mechanism of sIL-6R generation in MIA-MSLN cells, we used primers that specifically amplify the alternatively spliced mRNA and tried to detect it by real-time polymerase chain reaction. There were very low levels of this form in both cells (data not shown). Thus, the increase in sIL-6R in MIA-MSLN cells was not due to different levels of alternatively spliced IL-6R transcript. We then checked expression levels of the ADAM10 and ADAM17. mRNA expression of these two proteases was similarly high in both cells (data not shown). Treatment with a TACE (ADAM17) inhibitor TAPI-1 could clearly reduce sIL-6R in MIA-MSLN cells (Figure 5D) with a concomitant decrease in cell proliferation of these cells ($P < 0.01$, Figure 5E). The data indicates that MIA-MSLN cells have increased protease mediated cleavage of membrane IL-6R which might be responsible for an enhanced autocrine trans-signaling in combination with the autocrine IL-6 produced by these cells, helping them survive under growth factor devoid situations.

IL-6/sIL-6R trans-signaling may be responsible for the enhanced cell proliferation in MIA-MSLN cells

To clearly establish the functional significance of upregulated sIL-6R in MIA-MSLN cells, we used a sIL-6R-specific neutralizing antibody to block sIL-6R and examined both endogenous and exogenous IL-6-induced proliferation. Blocking the sIL-6R decreased MIA-MSLN cell viability by almost 25% ($P < 0.05$), whereas the isotype antibody had no effect (Figure 6A). Similarly, blocking sIL-6R also blocked the IL-6-induced proliferation of MIA-MSLN cells (Figure 6B).

Since IL-6 alone could not induce proliferation of low-MSLN-expressing MIA-V cells, we asked if this was due to lack of sIL-6R in these cells. So, we treated MIA-V/MIA-MSLN cells with a cocktail of exogenous rIL-6 and recombinant sIL-6R (rsIL-6R). The rIL-6/rsIL-6R mixture indeed induced a significant increase in proliferation of the MIA-V cells (~ 1.5 times in 3 days, $P < 0.01$, Figure 6C). These data demonstrate that IL-6/sIL-6R trans-signaling was involved in the MIA-V cell proliferation/survival as well. Expectedly, rIL-6/rsIL-6R induced increased proliferation in MIA-MSLN cells to a greater extent (~ 1.9 times in 3 days, $P < 0.01$, Figure 6C). Most importantly, blocking sIL-6R with sIL-6R-specific neutralizing antibody completely abolished this growth-promoting effect ($P < 0.01$, Figure 6C) but a matched isotype control antibody could not block the effect. Altogether, the data clearly established IL-6 trans-signaling to be a major factor affecting survival/proliferation of MSLN-expressing PC cells.

MSLN/IL-6 axis provides a major survival signal in PC cells

MSLN has been described to affect survival of cancer cells under various conditions as well as support other tumorigenic properties (2–4,29,30). To clearly establish a pro-proliferative role of MSLN/IL-6 in an extended PC cell line panel, we chose five different PC cell lines based on our MSLN/IL-6 expression screening results shown in Table I to examine their survival dependence on both MSLN and IL-6. As shown in Figure 7A, three of the cell lines expressed high MSLN and high IL-6 (Hs766T/PL-45/BxPC-3), one MSLN high but IL-6-low (AsPC-1) and one (HPDE) which was low in both MSLN and IL-6. We first used siRNA against MSLN to determine the importance of MSLN in cell survival. Since the HPDE and PL45 cell lines were generally unhealthy after 5 days in serum-free media along with the effect of the transfection reagent, these were excluded from the analysis. As shown in Figure 7B, MSLN siRNA could effectively block the growth of all three MSLN high cells irrespective of their IL-6 status. We also generated a stable MSLN knockdown AsPC-1 cell (AsPC-shMSLN) and tested the proliferation of these cells compared with the control AsPC-1 WT, vector control (AsPC-V) and AsPC-shGFP (non-specific shRNA control) cells. As shown in Figure 7C, the MSLN knockdown stable cells had a significantly decreased proliferation rate when compared with all the controls. Again, the pro-survival/proliferative role of MSLN was demonstrated in multiple PC cells.

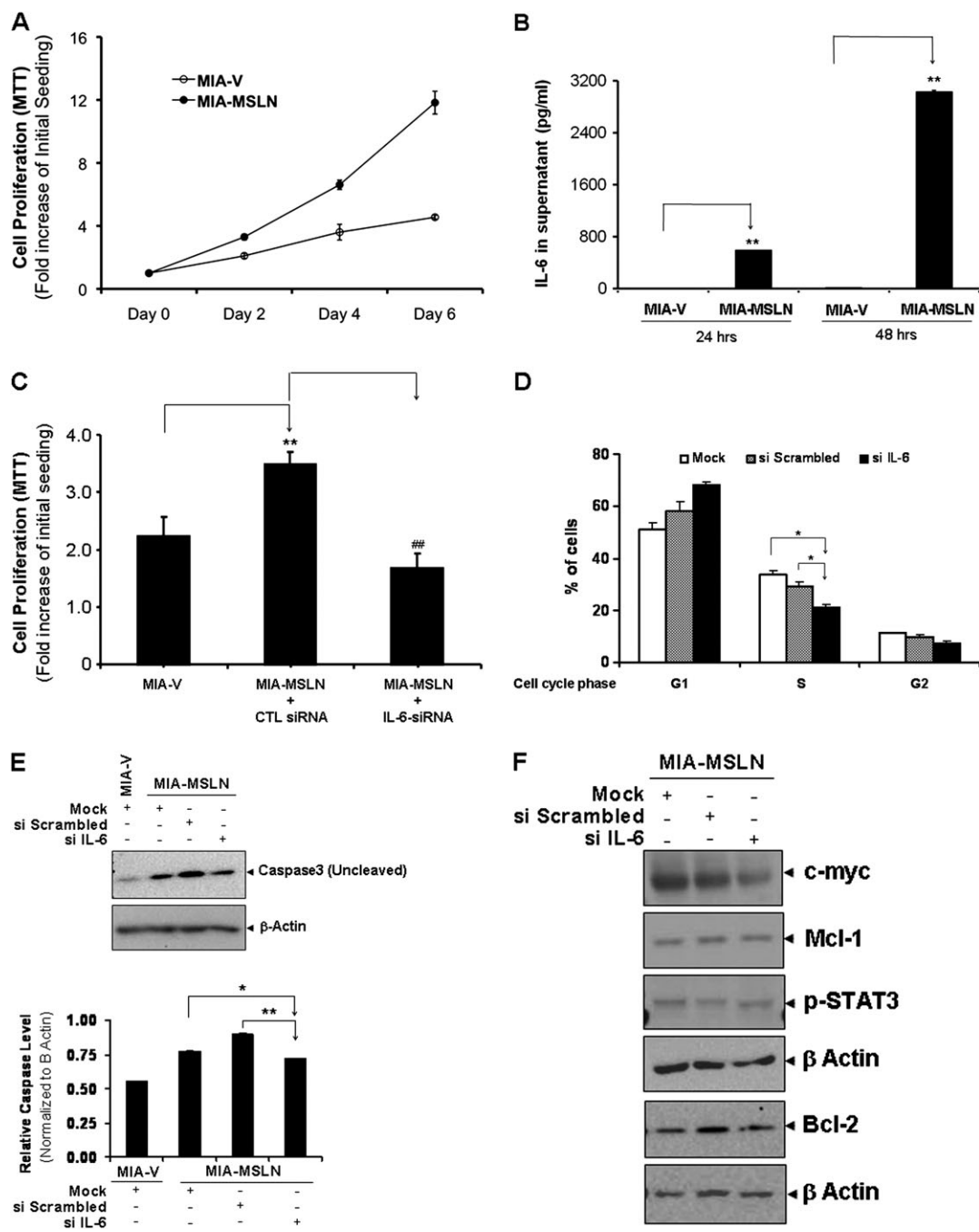


Fig. 4. IL-6 is an autocrine growth and survival factor for the MIA-MSLN cells. (A) Overexpression of MSLN promotes PC cell proliferation in serum-free conditions. MIA-MSLN and control MIA-V cells were seeded in 96-well plates (2×10^3 cells per well), serum starved (0% FBS) for 24 h before changing to fresh serum-free medium and cultured for 6 days. Viability was measured with MTT. Relative increase in viability was measured by dividing viability at a time point by viability of same cells at day 0 (day after plating) and is plotted along Y-axis. Data plotted show mean of triplicate wells. Proliferation after initial starvation followed by low serum supplementation was performed several times, serum-free survival was also performed multiple times, and data shown is a representative one. (B) Serum starvation increases IL-6 production by MIA-MSLN but not by MIA-V cells. MIA-V or MIA-MSLN cells (4×10^6) were plated in T75 flasks and cultured till 90% confluent. Growth medium was then replaced by serum-free medium and supernatants were collected after 24 and 48 h and assayed for IL-6 using the Luminex-based IL-6 assay kit. Values on Y-axis show the amount of IL-6 in pg/ml, bars denoting SD of duplicate data. (C) IL-6 siRNA reduced MIA-MSLN cell proliferation. MIA-V and MIA-MSLN cells were transfected in six-well plates using a pool of four IL-6-specific siRNAs or a negative control pool of scrambled siRNAs. At 24 h after the transfection, cells were trypsinized, counted and seeded in 96-well plates (2×10^3 cells per well), serum starved (0% FBS) for 24 h before changing to fresh medium with 0.2% FBS and cultured for 2 days. Viability was measured with MTT. Relative increase in viability was measured by dividing viability at a time point by viability of same cells at day 0 (day after plating) and is plotted along Y-axis. Data plotted show mean of triplicate wells. *, # denote $P < 0.05$, and **, ## denote $P < 0.01$, compared with controls, *t*-test. Experiment was performed several times using various serum conditions with similar results shown is a representative data. (D) IL-6 siRNA reduced cell cycle distribution of MIA-MSLN cells. MIA-MSLN cells treated with IL-6-specific siRNA as previously were allowed to grow in serum-free media for 24 h after initial growth media replenishing for 12 h posttransfection and collected for Propidium Iodide (PI) staining. The numbers of cells in each phase are plotted along the Y-axis. (E) IL-6 siRNA transfected and control MIA-MSLN cells were continued in culture for 96 h and subjected to Caspase3 activation detection by western blot. (F) In order to see which IL-6/stat3 regulated genes were affected by IL-6 siRNA treatment, control and siIL-6 treated MIA-MSLN cells were subject to western blot detection of various IL-6/stat3 regulated genes.

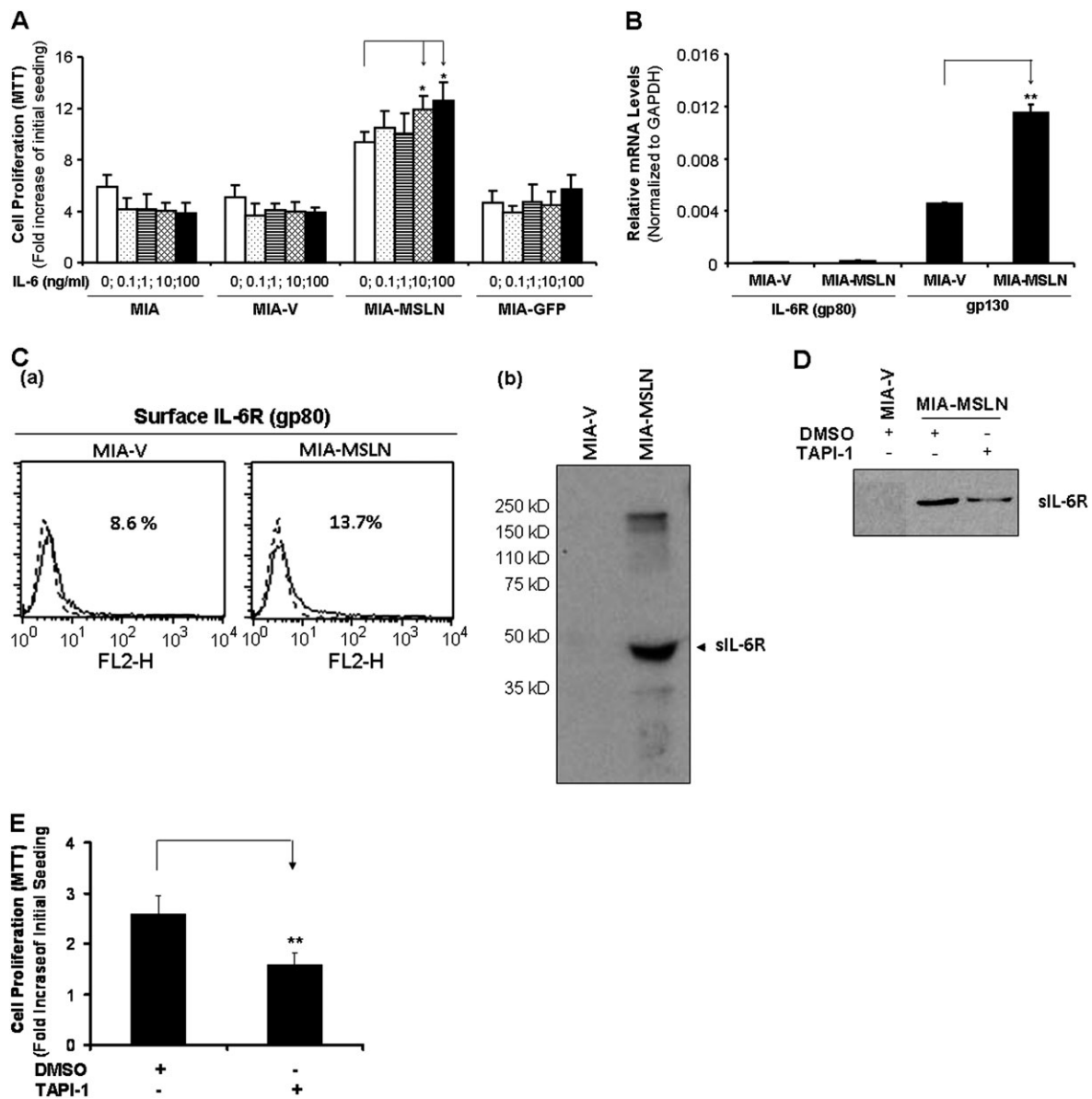


Fig. 5. Auto/paracrine IL-6 trans-signaling is enhanced in MIA-MSLN cells through upregulated soluble IL-6 receptors. **(A)** Exogenous rIL-6 induces proliferation in MIA-MSLN cells. MIA-MSLN and control MIA-V cells were seeded in 96-well plates (2×10^3 cells per well), serum starved (0% FBS) for 24 h and treated with indicated concentrations of IL-6 in 0.2% FBS containing medium for 3 days. Viability was measured with MTT. Relative increase in viability was measured by dividing viability at a time point by viability of same cells at day 0 (day after plating) and is plotted along Y-axis. Data plotted show mean of triplicate wells and is representative of at least two similar experiments. **(B)** IL-6 receptor gp80 and gp130 expression patterns in MIA-V and MIA-MSLN cells. IL-6 receptor gp80 and gp130 mRNA expression levels were determined by using real-time polymerase chain reaction in both MIA-V and MIA-MSLN cells. Y-axis shows GAPDH-normalized mRNA levels for gp80 and gp130 in MIA-V and MIA-MSLN cells. Relative mRNA level is presented as $2^{-[C_t(\text{GAPDH}) - C_t(\text{IL-6})]}$. The bars denote SD of duplicate data. **(C)** Cell surface IL-6R (gp80) and soluble IL-6 receptor (sIL-6R) expression patterns in MIA-V and MIA-MSLN cells. **(a)** Cell surface gp80 expression was analyzed by FACS using anti-gp80 antibody. The results are depicted as histograms, the percentage denotes the positive cell population. sIL-6R expression in MIA-V and MIA-MSLN supernatants **(b)** was analyzed by western blot with anti-IL-6R antibody. *, # denote $P < 0.05$, and **, ## denote $P < 0.01$, compared with controls, *t*-test. **(D)** Effect of ADAM inhibitor TAPI-1 on the generation of sIL-6R in MIA-MSLN cells. Supernatant collected after 48 h treatment with the indicated concentrations of TAPI-1 or dimethyl sulfoxide were concentrated and used to detect the 50 kD sIL-6R band by western. **(E)** Treatment with TAPI-1 concurrently decreased the cell proliferation of MIA-MSLN cells as indicated. Relative increase in viability was measured by dividing viability at a time point by viability of same cells at day 0 (day after plating) and is plotted along Y-axis. Data plotted show mean of triplicate wells. *, # denote $P < 0.05$, and **, ## denote $P < 0.01$, compared with controls, *t*-test.

To examine another important function that MSLN might confer to PC cells, anchorage-independent growth properties were examined. In addition, IL-6 has been found to be supportive of anchorage-independent growth in various cancers. Here, we look at the cell lines with both high MSLN and high IL-6 expression and found that they had high propensity to grow in spheroid cultures forming much bigger colonies in ultra-low attachment plates than the HPDE cells (Figure 7D). Therefore, it seems MSLN and IL-6 support cell growth in

reduced serum and apoptosis inducing conditions and the growth promotion stems from increased survival as well as increased cell cycle progression under these conditions (3,20). The current data combined with our (data not shown) and others' data (4) that MSLN overexpression leads to resistance to anoikis also point toward a complex role of MSLN in PC survival. We also found that BxPC3 has limited ability to grow on soft agar (data not shown) but easily form colonies under anchorage-independent assay (Figure 7D) in low

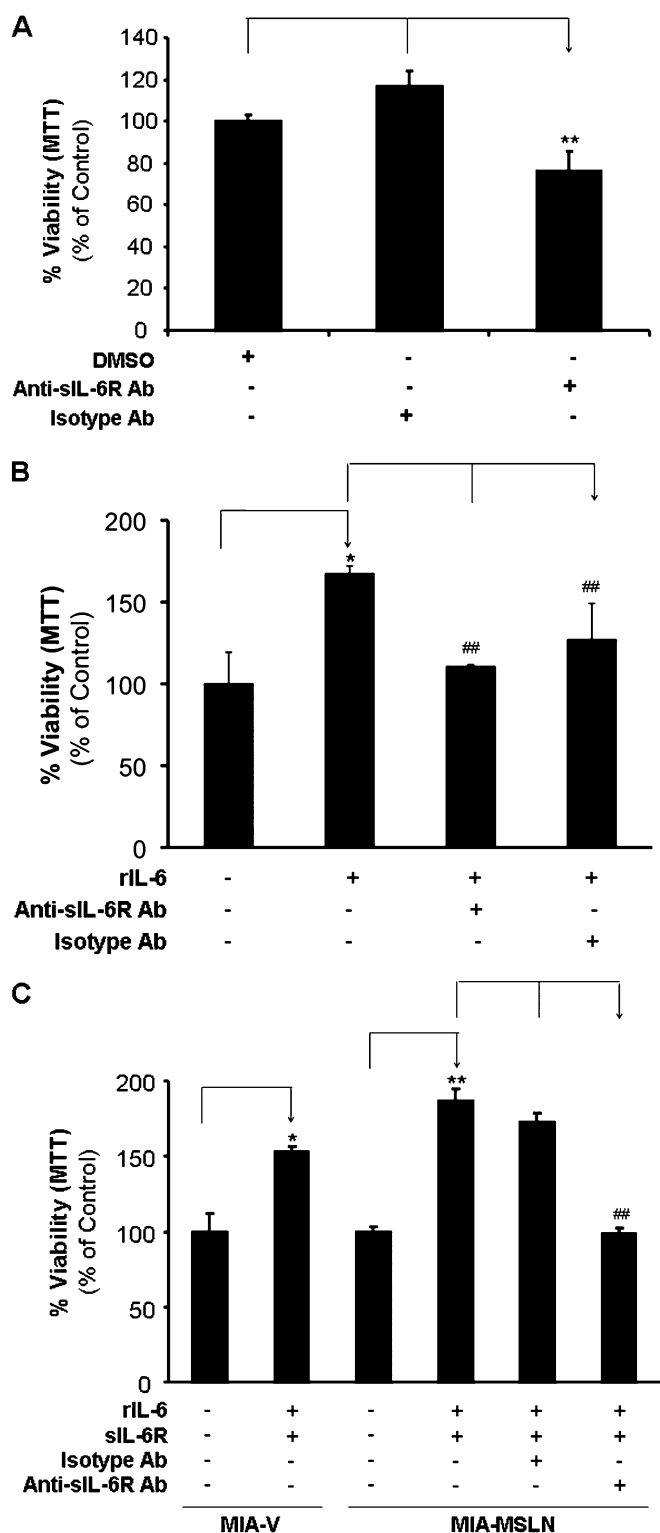


Fig. 6. Blocking the IL-6/sIL-6R trans-signaling axis affects the growth/survival of MSLN expressing PC cell proliferation. (A) sIL-6R antibody blocking can reduce the endogenous IL-6-induced proliferation of MIA-MSLN cells. MIA-MSLN cells were seeded in 96-well plates (2×10^3 cells per well), serum starved (0% FBS) for 24 h with or without anti-sIL-6R or isotype control antibody. The cells were then treated with 0.2% FBS containing medium for 3 days. Viability was measured with MTT. Relative viability was measured by dividing viability after a treatment by viability of same cells without treatment (or dimethyl sulfoxide treated) and is plotted along Y-axis. Data plotted show mean of triplicate wells and is representative of at least two similar experiments. (B). Soluble IL-6R antibody blocking can reduce the exogenous IL-6-induced

attachment plates. Furthermore, when IL-6 is silenced in BxPC3 cells, the size and numbers of spheroids formed were visibly reduced compared with scramble siRNA treated BxPC-3 cells shown in Figure 7E, (i) MSLN siRNA almost obliterated the formation of spheroids completely. Besides, comparing the viabilities of these differentially treated cells, also clearly showed that both siIL-6 and siMSLN reduced the anchorage-independent growth of BxPC3 cells although the effect of siMSLN was apparently much greater (Figure 7E, ii). Thus, this study is significant in determining the role of IL-6 in MSLN-induced tumor progression.

To further examine whether IL-6 is involved in MSLN-supported tumorigenic properties, the effect of rIL-6 treatment or IL-6 siRNA mediated blocking were tested in several naturally MSLN-overexpressing cells. Shown in Figure 7F, when cells were treated with recombinant IL-6, all the three MSLN/IL-6 high cells (Hs766T/PL45/BxPC3) had increased proliferation by 17, 23 and 83% ($P < 0.05$, $P < 0.01$, $P < 0.01$ respectively, Figure 7F). Although IL-6/sIL-6R combination could also increase proliferation in two of these cells, it did not increase proliferation beyond that induced by IL-6 alone. This result again pointed toward IL-6 as an autocrine growth factor for MSLN high-expressing cells and underscores the importance of the MSLN/IL-6 axis in PC cell survival/proliferation. In addition, siRNA against IL-6 was also used to determine whether it can block proliferation of these cells. Interestingly, of the two MSLN/IL-6 high cells, IL-6 siRNA treatment significantly reduced ability of BxPC3 cells to grow but did not affect growth of Hs766T cells. While the MSLN-high, IL-6-low AsPC-1 cells were also not affected by IL-6 siRNA (Figure 7G). Altogether, our data with these various cell lines indicate a very important survival axis of MSLN/IL-6 in the tumorigenic behavior of PC cells.

Discussion

The present study clearly indicates that MSLN overexpression leads to increased IL-6 production, which in a positive manner regulates survival and proliferation of PC cells under serum-reduced and anchorage-independent conditions. The high correlation of MSLN expression in the tumor tissue of PC patients with the serum IL-6 level indicated a possible mechanism of IL-6 induction in PC cells. The MSLN/IL-6 mRNA data from multiple PC cell lines also corroborated the same notion. In several cell lines with endogenously high MSLN expression, either MSLN or IL-6 was knocked down using siRNA, and we found that reduced MSLN or IL-6 expression leads to reduced cell growth and reduced formation of spheroids. These data make apparent the fact that MSLN and IL-6 positively regulate the survival/proliferation of MSLN-expressing PC cells, which makes MSLN an ideal target for intervention in those patients with high MSLN-expressing tumors. MSLN-induced constitutive NF- κ B activation seemed to be responsible for the elevated IL-6 production. We also found that MIA-MSLN cells had minimal membrane IL-6R expression, but increased sIL-6R levels, presumably through

proliferation of MIA-MSLN cells. MIA-MSLN cells were serum-starved (0% FBS) for 24 h with or without anti-sIL-6R or isotype control antibody and then treated with a cocktail of rIL-6/rsIL-6R in 0.2% FBS containing medium for 3 days. Viability was measured with MTT. Relative viability was measured by dividing viability of treated cells (treated with rIL-6/rsIL-6R cocktail with or without anti-sIL-6R antibody blocking) by that of untreated cells and is plotted along Y-axis. Data plotted show mean of triplicate wells. (C) IL6/sIL-6R trans-signaling axis is operative in MIA cell proliferation. Both MIA-V and MIA-MSLN cells were serum starved (0% FBS) for 24 h with or without anti-sIL-6R or isotype control antibody and then treated with a cocktail of rIL-6/rsIL-6R in 0.2% FBS containing media for 3 days. Viability was measured with MTT. Relative increase in viability was measured by dividing viability of treated cells (treated with rIL-6/rsIL-6R cocktail with or without anti-sIL-6R antibody blocking) by that of untreated cells and is plotted along Y-axis. Data plotted show mean of triplicate wells. *, # denote $P < 0.05$, and **, ## denote $P < 0.01$, compared with controls, *t*-test.

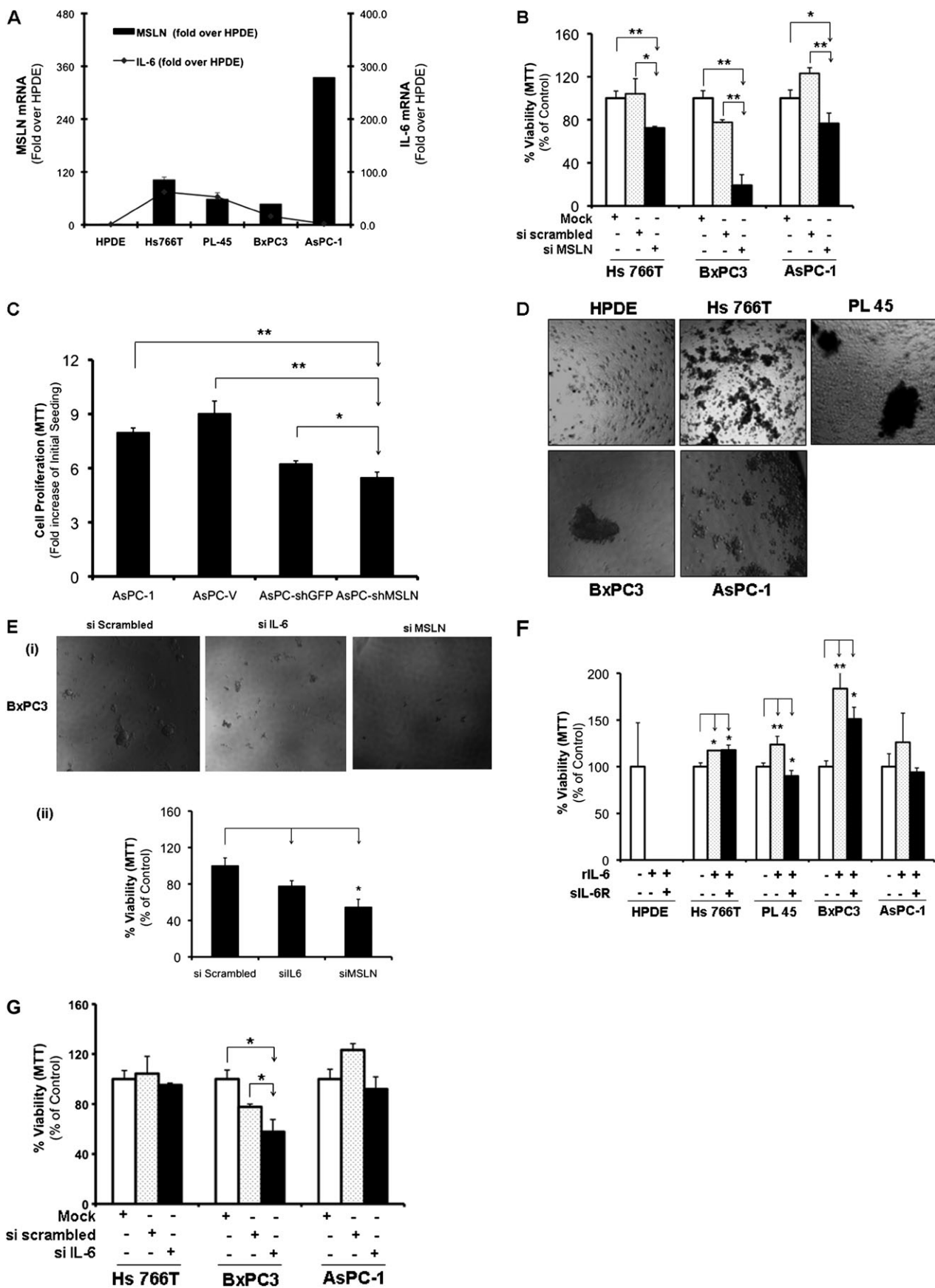


Fig. 7. MSLN/IL-6 axis provides a major survival signal in PC cells affecting growth under both anchorage-dependent and independent conditions. (A) Relative MSLN and IL-6 mRNA expression in selected PC cells. Total mRNA from the cell lines were reverse transcribed and tested for MSLN/IL-6 expression. The left hand side Y-axis denotes MSLN mRNA levels in each cell line normalized to the GAPDH mRNA level. Relative mRNA level is presented as $2^{-C_t(\text{GAPDH}) - C_t(\text{MSLN/IL-6})}$.

Downloaded from https://academic.oup.com/carcin/article/32/7/1013/2733278 by guest on 15 March 2021

intramembrane cleavage sIL-6R as TAPI-1, a TACE inhibitor was able to block it. The overexpression of IL-6 and the increased sIL-6R in MSLN overexpressing cells were found to be supportive of its survival and proliferation, under anchorage dependent as well as independent conditions as blocking the IL-6/sIL-6R axis using antibodies or IL-6 siRNAs decreased viability and/or cell cycle progression. Apoptosis induced by long-term sIL-6 treatment and ability of exogenous IL-6 to stimulate growth in the MIA-MSLN cells was also indicative of its IL-6-dependent survival and proliferation.

We found constitutive activation of NF- κ B in MIA-MSLN cells leads to enhanced production of IL-6. Activated NF- κ B has previously been shown to increase IL-6 production in a variety of cancers (23). However, our data showing MSLN overexpression leads to NF- κ B activation and in turn to IL-6 production are novel findings. Data from our lab indicate MSLN-expressing cells have increased integrin expression (data not shown) as also enhanced integrin-mediated signaling e.g. through FAK, src activation. We believe this to be a potential mechanism of NF- κ B activation in these cells. Pancreatic stellate cells, key players in pancreatic neoplasm, produce increased IL-6 in an NF- κ B-dependent manner through interaction with fibrinogen via integrin α V/ β 3 and/or integrin α V/ β 1 (31). It is noteworthy to mention here that the MSLN overexpressing cells, when grown on matrigel-coated plates, had even further increased NF- κ B activation as well as IL-6 production (data not shown) indicating the probable involvement of this pathway.

Previous reports implicated autocrine tumor necrosis factor (TNF)- α in IL-6 production by ovarian cancer cells (32). Our finding that MSLN overexpressing cells secrete increased amounts of TNF- α (data not shown) raises the possibility of a similar axis in MSLN-positive PC cells. There are suggestions that IL-6 in presence of TNF- α , but not alone, could induce fibroblast proliferation (33). Thus, it is a possibility that the presence of both TNF- α and IL-6 in the MIA-MSLN cells make them responsive to IL-6. The increase in both sIL-6R and TNF- α by these cells indicated an increased activity of the enzyme TACE (ADAM17) reported responsible for the generation of (34–36) these. In fact, a TACE inhibitor successfully reduced sIL-6R level in these cells.

Although the IL-6 receptor gp80 mRNA was not significantly increased in MIA-MSLN cells, there was a significant, albeit small, increase in the gp130 level (Figure 5B). gp130 signaling in concert with sIL-6R was found to be more important in IL-6 signaling than the membrane-bound IL-6R in hepatoma (37). The discovery that MIA-MSLN cells have increased sIL-6R is significant. This probably facilitates the IL-6/sIL-6R trans-signaling axis in MSLN overexpressing PC. In fact, blocking IL-6/sIL-6R activity using sIL-6R-specific antibodies reduced MIA-MSLN cell viability, although to a lesser extent than using IL-6 siRNA. This raises another possibility, that IL-6 is acting as an intracrine cytokine and hence, its action could not be as

efficiently blocked by blocking receptors, as has been previously suggested (24,25). Furthermore, our finding that the MIA-V cells proliferate more rapidly following a combined rIL-6/rsIL-6R treatment underscores the importance of IL-6 trans-signaling in PC. Our observation that the MSLN/IL-6 survival axis operates in multiple PC cells makes it a viable target for drug discovery. It becomes more important on the pretext that there is huge infiltration of IL-6-producing cells, particularly macrophages (9), during various stages of PC. Cells-expressing MSLN could be more effectively using this abundant cytokine to support their survival. Interestingly, IL-6 trans-signaling is found to induce growth and angiogenesis in mesothelioma, another cancer with high MSLN expression (5). The report (38) that IL-6 was elevated in mesothelioma patients with high soluble MSLN-related peptides levels also points toward a possible role of MSLN in increased IL-6 production. Unstimulated human peritoneal mesothelial cells under growth-arrested conditions released IL-6 in a time-dependent manner (39,40), which was further increased by IL-1 β treatment. Looking at the constitutive and inducible (e.g. serum starvation, growth on matrigel) IL-6 in MIA-MSLN cells together with the documented role of IL-6 production/usage in mesothelial cells leads one to speculate a possible role of MSLN in co-coordinating, balancing and augmenting inflammatory responses. This might well be important in context of all cancers overexpressing MSLN, including lung cancer, mesothelioma and PC, all of which have an inflammatory (23) beginning, which culminates into full-fledged neoplasm presumably through upregulation of MSLN.

The exact role IL-6 plays in cancer pathogenesis, particularly its role in proliferation, is not fully understood. Several articles have shown (5,24–27) that IL-6 positively regulates proliferation in epithelial cancer cells (41). Lee *et al.* (42) showed that during early passages, IL-6 actually suppressed the growth of prostate cancer cell lines, but in later passages, with emergence of androgen receptor, cells became sensitive to IL-6-induced proliferation. On the contrary, a recent paper very clearly shows that during early phases of fibroblast transformation by oncogenic stress, IL-6 actually helps cells survive oncogene-induced senescence by inhibiting or slowing down the proliferation of these cells (43). The pleiotropic effect of IL-6 on cancer cell proliferation has thus been suggested to be context dependent. In a very recent paper, for example, Galvez *et al.* (44) clearly show that IL-6 plays an important role in the ability of cells to grow under nutrient low conditions *in vitro* and *in vivo*. We believe this is the same scenario as that in the current study. MIA PaCa-2, like other PC cells, is a mKRAS-transformed cell and we find IL-6/sIL-6R trans-signaling increases its survival under low serum conditions. The fact that MSLN is upregulated late in the multistep model of PC pathogenesis underscores its role in cells where a majority of genetic changes (KRAS mutation, p53 mutation, p16 mutation, SMAD4 deletion) or a major one (e.g. KRAS) have already set in, and fits very

C.(MSLN)]. The bars denote SD of duplicate data. Line graph represents the IL-6 mRNA in the same cell lines and the right hand side Y-axis indicates normalized IL-6 levels. (B) Effect of blocking MSLN on cell growth of multiple PC cells. Hs766T, BxPC3, both expressing MSLN/IL-6 and AsPC-1 with high MSLN and low IL-6 were treated with pools of MSLN-specific siRNA or non-targeting scrambled siRNA and plated as per reverse transcription protocol in 96-well plates in triplicates. After 36 h, complete media was replaced by serum-free media and then after another 24 h by 0.2% serum containing media and cultured for 5 days. Relative viability was measured by dividing viability of treated cells (treated with MSLN/scrambled siRNA) by that of mock-treated cells using MTT and is plotted along Y-axis. Data plotted show mean of triplicate wells. *, denote $P < 0.05$, and **, denote $P < 0.01$, compared with controls, *t*-test. (C) Stable MSLN-silenced AsPC-shMSLN cells and proliferation. Cells were seeded in 96-well plates (2×10^3 cells per well), serum starved (0% FBS) for 24 h before changing to fresh 0.2% FBS medium and cultured for 6 days. Viability was measured with MTT. Relative increase in viability was measured by dividing viability at a time point by viability of same cells at day 0 (day after plating) and is plotted along Y-axis. Data plotted show mean of triplicate wells. (D) Ability of MSLN-expressing cells to grow under anchorage-independent conditions. Cells were plated in ultra-low attachment plates and allowed to grow spheroid cultures for 8 days and then photographed. Shown are representative wells for each cell. (E) At 36 h posttransfection, BxPC3 cells treated with pools of MSLN/IL-6-specific siRNA or non-targeting scrambled siRNA in six-well plates were trypsinized and plated at 6000 cells per well of ultra-low attachment 96-well plates and cultured for 5 days before being photographed. (i) Spheroid colonies formed by BxPC3 \pm IL-6/MSLN/scrambled siRNAs. (ii) Viability was measured by MTT. Relative viability was measured by dividing viability of treated cells (treated with MSLN/IL-6/scrambled siRNA) by that of mock-treated cells and is plotted along Y-axis. Data plotted show mean of triplicate wells. *, # denote $P < 0.05$, and **, ## denote $P < 0.01$, compared with controls, *t*-test. (F) Exogenous rIL-6 induces proliferation in MSLN-expressing PC cells. Cells were seeded in 96-well plates (3×10^3 cells per well), serum starved (0% FBS) for 24 h and treated with IL-6 (100 ng/ml) \pm sIL-6R (50 μ g/ml) in serum-free medium for 5 days. Relative viability was measured by dividing viability after any treatment by viability of untreated cells by MTT and is plotted along Y-axis. Data plotted show mean of triplicate wells. Effect of blocking IL-6 and MSLN on growth of MSLN/IL-6-expressing cells under anchorage-dependent (G) conditions. Cell lines were treated with pools of IL-6-specific siRNA or non-targeting scrambled siRNA and plated as per reverse transcription protocol in 96-well plates in triplicates. After 36 h, serum-free media were added and then after another 24 h using 0.2% serum-containing media and cultured for 5 days. Relative viability was measured by dividing viability of treated cells (treated with IL-6/scrambled siRNA) by that of mock-treated cells using MTT and is plotted along Y-axis. Data plotted show mean of triplicate wells. *, # denote $P < 0.05$, and **, ## denote $P < 0.01$, compared with controls, *t*-test.

well in our model of auto/paracrine IL-6 signaling stimulated survival/proliferation. In fact, simultaneous disruption of p53 and Rb pathway by SV40 early genomic region and introduction of hTERT and KRAS(V12) into human ovarian surface epithelial cells immortalized and transformed these cells with increased expression of MSLN, CA125 and several cytokines including IL-6 in an NF- κ B-mediated manner (45). Oncogenic transformation has always seen the upregulation of MSLN in multiple-independent studies and across species (30,46). It remains to be seen though, whether MSLN-induced IL-6 in these contexts, i.e. during or immediately after oncogenic transformation supports or delays cell cycle progression. We are precisely examining these now, using cells expressing mutant KRAS \pm other mutations at various stages of transformation.

In the present study, we have clearly established that blocking IL-6 not only delays S phase progression but also eventually leads to apoptosis indicating IL-6 might be important for survival of MSLN-expressing PC cells. The overall consensus that IL-6 increases survival of pancreatic cells, especially under stress, stands established (10,12–14). In this context, the fact that MSLN increases IL-6 expression may help explain an across-the-board overexpression of MSLN in PC. Further study will help in the formulation of new rationales for combined therapy coupling anti-MSLN immunotherapy, IL-6 blockade (47) and/or radiation/chemotherapy for effective clearance of residual disease in MSLN-overexpressing tumors.

Funding

This work was supported in part by Dan L Duncan Cancer Center pilot grant from Baylor College of Medicine (BCM) and the National Institutes of Health Grant CA140828 for Q.Y.

Conflict of Interest Statement: None declared.

References

- Hassan,R. *et al.* (2004) Mesothelin: a new target for immunotherapy. *Clin. Cancer Res.*, **10**, 3937–3942.
- Li,M. *et al.* (2008) Mesothelin is a malignant factor and therapeutic vaccine target for pancreatic cancer. *Mol. Cancer Ther.*, **7**, 286–296.
- Bharadwaj,U. *et al.* (2008) Mesothelin-induced pancreatic cancer cell proliferation involves alteration of cyclin E via activation of signal transducer and activator of transcription protein 3. *Mol. Cancer Res.*, **6**, 1755–1765.
- Uehara,N. *et al.* (2008) Mesothelin promotes anchorage-independent growth and prevents anoikis via extracellular signal-regulated kinase signaling pathway in human breast cancer cells. *Mol. Cancer Res.*, **6**, 186–193.
- Adachi,Y. *et al.* (2006) Interleukin-6 induces both cell growth and VEGF production in malignant mesotheliomas. *Int. J. Cancer.*, **119**, 1303–1311.
- Yeh,H.H. *et al.* (2006) Autocrine IL-6-induced Stat3 activation contributes to the pathogenesis of lung adenocarcinoma and malignant pleural effusion. *Oncogene*, **25**, 4300–4309.
- Cavarretta,I.T. *et al.* (2007) The antiapoptotic effect of IL-6 autocrine loop in a cellular model of advanced prostate cancer is mediated by Mcl-1. *Oncogene*, **26**, 2822–2832.
- Lin,M.T. *et al.* (2001) IL-6 inhibits apoptosis and retains oxidative DNA lesions in human gastric cancer AGS cells through up-regulation of anti-apoptotic gene mcl-1. *Carcinogenesis*, **22**, 1947–1953.
- Hodge,D.R. *et al.* (2005) The role of IL-6 and STAT3 in inflammation and cancer. *Eur. J. Cancer.*, **41**, 2502–2512.
- Bellone,G. *et al.* (2006) Cytokine expression profile in human pancreatic carcinoma cells and in surgical specimens: implications for survival. *Cancer Immunol. Immunother.*, **55**, 684–698.
- Okada,S. *et al.* (1998) Elevated serum interleukin-6 levels in patients with pancreatic cancer. *Jpn. J. Clin. Oncol.*, **28**, 12–15.
- Lang,S.A. *et al.* (2007) Targeting heat shock protein 90 in pancreatic cancer impairs insulin-like growth factor-I receptor signaling, disrupts an interleukin-6/signal-transducer and activator of transcription 3/hypoxia-inducible factor-1 α autocrine loop, and reduces orthotopic tumor growth. *Clin. Cancer Res.*, **13**, 6459–6468.
- Friess,H. *et al.* (1999) Growth factors and cytokines in pancreatic carcinogenesis. *Ann. N. Y. Acad. Sci.*, **880**, 110–121.
- Miyamoto,Y. *et al.* (2001) Interleukin-6 inhibits radiation induced apoptosis in pancreatic cancer cells. *Anticancer Res.*, **21**, 2449–2456.
- Coussens,L.M. *et al.* (2002) Inflammation and cancer. *Nature*, **420**, 860–867.
- Naugler,W.E. *et al.* (2008) The wolf in sheep's clothing: the role of interleukin-6 in immunity, inflammation and cancer. *Trends Mol. Med.*, **14**, 109–119.
- Bollrath,J. *et al.* (2009) gp130-mediated Stat3 activation in enterocytes regulates cell survival and cell-cycle progression during colitis-associated tumorigenesis. *Cancer Cell*, **15**, 91–102.
- Bromberg,J. *et al.* (2009) Inflammation and cancer: IL-6 and STAT3 complete the link. *Cancer Cell*, **15**, 79–80.
- Fujino,S. *et al.* (1996) Interleukin 6 is an autocrine growth factor for normal human pleural mesothelial cells. *Am. J. Respir. Cell Mol. Biol.*, **14**, 508–515.
- Zhang,D. *et al.* (2011) Deficiency of the Erc/mesothelin gene ameliorates renal carcinogenesis in Tsc2 knockout mice. *Cancer Sci.*, **102**, 720–727.
- Bharadwaj,U. *et al.* (2007) Elevated interleukin-6 and G-CSF in human pancreatic cancer cell conditioned medium suppress dendritic cell differentiation and activation. *Cancer Res.*, **67**, 5479–5488.
- Ebrahimi,B. *et al.* (2004) Cytokines in pancreatic carcinoma: correlation with phenotypic characteristics and prognosis. *Cancer*, **101**, 2727–2736.
- Aggarwal,B.B. *et al.* (2006) Inflammation and cancer: how hot is the link? *Biochem. Pharmacol.*, **72**, 1605–1621.
- Alberti,L. *et al.* (2004) IL-6 as an intracrine growth factor for renal carcinoma cell lines. *Int. J. Cancer.*, **111**, 653–661.
- Bihl,M. *et al.* (1998) Proliferation of human non-small-cell lung cancer cell lines: role of interleukin-6. *Am. J. Respir. Cell Mol. Biol.*, **19**, 606–612.
- Nishimoto,N. *et al.* (1994) Oncostatin M, leukemia inhibitory factor, and interleukin 6 induce the proliferation of human plasmacytoma cells via the common signal transducer, gp130. *J. Exp. Med.*, **179**, 1343–1347.
- Okamoto,M. *et al.* (1997) Interleukin-6 as a paracrine and autocrine growth factor in human prostatic carcinoma cells *in vitro*. *Cancer Res.*, **57**, 141–146.
- Rose-John,S. *et al.* (2007) The IL-6/sIL-6R complex as a novel target for therapeutic approaches. *Expert Opin. Ther. Targets.*, **11**, 613–624.
- Cheng,W.F. *et al.* (2009) High mesothelin correlates with chemoresistance and poor survival in epithelial ovarian carcinoma. *Br. J. Cancer.*, **100**, 1144–1153.
- Cheng,W.F. *et al.* (2007) Generation and characterization of an ascitogenic mesothelin-expressing tumor model. *Cancer*, **110**, 420–431.
- Masamune,A. *et al.* (2009) Fibrinogen induces cytokine and collagen production in pancreatic stellate cells. *Gut*, **58**, 550–559.
- Kulbe,H. *et al.* (2007) The inflammatory cytokine tumor necrosis factor- α generates an autocrine tumor-promoting network in epithelial ovarian cancer cells. *Cancer Res.*, **67**, 585–592.
- Lee,H.G. *et al.* (1995) Peritoneal lavage fluids stimulate NIH3T3 fibroblast proliferation and contain increased tumour necrosis factor and IL-6 in experimental silica-induced rat peritonitis. *Clin. Exp. Immunol.*, **100**, 139–144.
- Althoff,K. *et al.* (2000) Shedding of interleukin-6 receptor and tumor necrosis factor α . Contribution of the stalk sequence to the cleavage pattern of transmembrane proteins. *Eur. J. Biochem.*, **267**, 2624–2631.
- Mullberg,J. *et al.* (1999) Generation and function of the soluble interleukin-6 receptor. *Biochem. Soc. Trans.*, **27**, 211–219.
- Matthews,V. *et al.* (2003) Cellular cholesterol depletion triggers shedding of the human interleukin-6 receptor by ADAM10 and ADAM17 (TACE). *J. Biol. Chem.*, **278**, 38829–38839.
- Varga,V.L. *et al.* (2001) gp130-specific antisense oligonucleotides inhibit IL-6 signal inducing junB mRNA transcription in the human hepatoma cell line, HepG2. *Cell Biol. Int.*, **25**, 835–840.
- Amati,M. *et al.* (2008) Assessment of biomarkers in asbestos-exposed workers as indicators of cancer risk. *Mutat. Res.*, **655**, 52–58.
- Topley,N. *et al.* (1993) Human peritoneal mesothelial cells synthesize interleukin-6: induction by IL-1 beta and TNF alpha. *Kidney Int.*, **43**, 226–233.
- Witowski,J. *et al.* (1996) Superinduction of IL-6 synthesis in human peritoneal mesothelial cells is related to the induction and stabilization of IL-6 mRNA. *Kidney Int.*, **50**, 1212–1223.
- Serve,H. *et al.* (1991) Studies on the interaction between interleukin 6 and human malignant nonhematopoietic cell lines. *Cancer Res.*, **51**, 3862–3866.
- Lee,E.J. *et al.* (2007) Expression profiling identifies microRNA signature in pancreatic cancer. *Int. J. Cancer.*, **120**, 1046–1054.
- Kuilman,T. *et al.* (2008) Oncogene-induced senescence relayed by an interleukin-dependent inflammatory network. *Cell*, **133**, 1019–1031.

44. Galvez, A.S. *et al.* (2009) Protein kinase Czeta represses the interleukin-6 promoter and impairs tumorigenesis *in vivo*. *Mol. Cell. Biol.*, **29**, 104–115.
45. Liu, J. *et al.* (2004) A genetically defined model for human ovarian cancer. *Cancer Res.*, **64**, 1655–1663.
46. Fukamachi, K. *et al.* (2009) An animal model of preclinical diagnosis of pancreatic ductal adenocarcinomas. *Biochem. Biophys. Res. Commun.*, **390**, 636–641.
47. Wallner, L. *et al.* (2006) Inhibition of interleukin-6 with CNTO328, an anti-interleukin-6 monoclonal antibody, inhibits conversion of androgen-dependent prostate cancer to an androgen-independent phenotype in orchidectomized mice. *Cancer Res.*, **66**, 3087–3095.

Received September 17, 2010; revised March 20, 2011;
accepted April 17, 2011